Quaternary International 311 (2013) 44–53

Contents lists available at ScienceDirect

Quaternary International

journal homepage: www.elsevier.com/locate/quaint

Quaternary glacial chronology of the Kanas River valley, Altai Mountains, China

Jingdong Zhao [a,*], Xiufeng Yin [a], Jonathan M. Harbor [b], Zhongping Lai [a], Shiyin Liu [a], Zhongqin Li [a]

[a] State Key Laboratory of Cryospheric Sciences, Cold and Arid Regions Environmental and Engineering Research Institute, Chinese Academy of Sciences, Lanzhou 730000, China
[b] Department of Earth, Atmospheric, and Planetary Sciences, Purdue University, West Lafayette, IN 47907, USA

ARTICLE INFO

Article history:
Available online 16 August 2013

ABSTRACT

The Kanas River originates on the southern slope of Youyi Peak, the largest center of modern glaciation in the Altai Mountains in Central Asia. Glaciers advanced and retreated repeatedly during Quaternary glacial–interglacial cycles in the Kanas River valley, and four moraine complexes and associated glaciofluvial deposits are preserved in the valley. Optically stimulated luminescence (OSL) dating has been used to determine ages of glaciofluvial deposits (sand lenses sandwiched between tills in moraines) using a single aliquot regenerative-dose (SAR) protocol. Based on dating results from this and previous studies (including ^{14}C, electron spin resonance (ESR) and OSL dates) and geomorphic relationships, the innermost moraine complex was concluded to deposit during the Little Ice Age (LIA), the second (Akekule) moraine complex was deposited during the Neoglacial, the third (Kanas) moraine complex was deposited during the last glacial cycle (marine oxygen isotope stage (MIS) 2–4) and the outermost set of moraines is MIS 6 in ages (penultimate glaciation). The Kanas moraine complex could be divided into three subsets (III_1, III_2 and III_3), with inferred ages of MIS 2, mid-MIS 3 and MIS 4, respectively, which is consistent with moraine records from other areas in Central Asia and climate reconstructions from the Guliya ice core. The glaciers in the Kanas valley at their maximum extents during the LIA, Neoglacial, last glaciation and penultimate glaciation were 13.8 km, 32 km, ~100 km, and ~120 km long, respectively.

1. Introduction

Alpine glaciers are highly sensitive to climate change, and advance or retreat rapidly with changes in temperature and/or precipitation. Glaciers are also very important and active geomorphic agents and are responsible for producing some of the most spectacular landforms and landscapes on Earth (e.g. cirques, horns, arêtes, hanging valleys, glacial troughs, roche moutonnées, polished bedrock, lateral moraines, end moraines, hummocky moraines and other features) (Embleton and King, 1975; Benn and Evans, 2010). Glacial landforms are a direct imprint of past glacial fluctuations and represent important archives of past climatic information. Studies of these landforms can provide insights into the nature of the ancient glacier fluctuations and offer essential information for reconstruction of paleoenvironments (Shi et al., 2006, 2011). Alpine glaciers advanced and retreated dramatically during Quaternary glacial–interglacial cycles, and glacial successions occur in valleys, basins and on piedmonts in glaciated regions throughout world (Ehlers et al., 2011). Dating these glacial landforms is a fundamental requirement in studying Quaternary glaciations and reconstructing past climates. Dating techniques, including optically stimulated luminescence (OSL), electron spin resonance (ESR) and cosmogenic radionuclides (CRN) are now widely used to determine the ages of glacial landforms and sediments (e.g. Yi et al., 2002; Zhou et al., 2002a, b; 2007; Owen et al., 2002b, 2003; Xu and Zhou, 2009; Zhao et al., 2009, 2012; Ou et al., 2010; Xu et al., 2010; Heyman et al., 2011; Wang et al., 2011, 2013; Fu et al., 2013), which has allowed for significant advances in research on the pattern and timing of Quaternary glaciations in China (Shi et al., 2011; Zhao et al., 2011).

The Altai Mountains are a major mountain system in Central Asia, stretching about 2000 km from west (West Siberian in Russia) to east (Mongolia). The southern slope of the middle segment of the Altai Mountains (45°47′–49°10′N, 85°27′–91°01′E) is about 500 km long and is located in the northern part of the Xinjiang Uigur Autonomous Region. This mountain system includes many East-

* Corresponding author.
E-mail address: jdzhao@lzb.ac.cn (J. Zhao).

1040-6182/$ – see front matter © 2013 Elsevier Ltd and INQUA. All rights reserved.
http://dx.doi.org/10.1016/j.quaint.2013.07.047

West trending mountain ranges, with the highest peak being Youyi Peak (4374 m asl). The Altai Mountains were extensively and repeatedly glaciated during the Quaternary and glacial landforms are well preserved in valleys and on piedmonts. Dating these landforms provides a way to reconstruct the temporal and spatial variation of past glaciers in this mountain system for comparison with other mountain ranges in Central Asia and the global record of glaciations.

Quaternary glacial landforms and glaciations in the Kanas River valley have been studied since the 1980s (Liu and Wang, 1983; Cui et al., 1992). Early researchers provided valuable insight into the geomorphology and deposits, but were not able to closely constrain the ages of glacial landforms and sediments because of the lack of well-developed absolute dating techniques at that time. Recent work has begun to provide constraints on some of the landforms in this valley, and Xu et al. (2009) have provided four initial OSL ages for one moraine complex in the valley named locally as the Kanas glaciation. However, controversy over these dates compared with the climatic record provided by the Guliya ice core in the West Kunlun Mountains (Thompson et al., 1997; Yao et al., 1997) and the RM core in the eastern Qinghai-Xizang Plateau (Wu et al., 2000) indicates that more extensive dating of this moraine complex and other moraines in the valley is needed to refine the chronology. Thus, we used OSL dating to determine the ages of lateral moraines in the main glacial trough and glacial landforms and sediments of the Kanas glaciation. This paper describes the Quaternary glacial landforms in the Kanas Valley and synthesizes new OSL data with previous dating results (^{14}C, OSL and ESR) to provide new insight into the timing of Quaternary glaciations and glacial landform evolution in this valley.

2. Regional setting

The Kanas River originates on the southern slope of Youyi Peak, which is located on the border between China, Mongolia and Russia. The Kanas River is about 125 km long and flows southwestward to the Burqin River and is a very important secondary tributary of the Irtysh River. Youyi Peak and several other peaks with altitudes of more than 4000 m form the largest center of modern glaciation in the Altai Mountains. There are 210 active modern glaciers in the Kanas River valley with equilibrium-line altitudes (ELA) between 3020 and 3360 m asl. Types of glaciers include hanging glaciers, cirque glaciers, single valley glaciers and compound valley glaciers, with a total area of about 209.5 km^2 and an ice volume of about 13.34 km^3 (Liu et al., 1982). Three valley glaciers with their lengths of more than 5 km are present in this valley, most notably the Kanas glacier, which is a compound valley glacier with several tributaries. In 1980, the Kanas glacier was about 10.8 km long, had an area of about 30 km^2 and an ice volume of about 3.92 km^3, and had its terminus at 2416 m asl (Liu et al., 1982). We observed that the terminus of the Kanas glacier in 2009 is at about 2460 m asl, which is more than 40 m higher than the 1980 position as a result of about 800 m of glacier retreat.

The climate of the Altai Mountains is dominated by mid-latitude westerlies, with precipitation directly influenced by the westerly circulation. A cold anticyclone typically develops during the winter over mid-Siberia and Mongolia as the primary control on the winter climate of the Altai Mountains. Occasionally, a polar air mass invades this area along the Irtysh River valley, resulting in low temperatures and snowfall in the mountainous area. Commonly, snowfall makes up 45–50% of the total annual precipitation, and the snow depth is 1.5–2.0 m in areas above 2000 m asl. Based on the snow pit data from the Kanas glacier, the annual precipitation at the ELA is 700–800 mm water equivalent (Liu et al., 1982), and meteorological data from the Altai Meteorological Station, with an environmental lapse rate of ~0.59 °C/100 m, indicating that the mean annual temperature at the ELA is about −7 to −8 °C (Wang et al., 1983).

3. Glacial landforms

Glacial erosional and depositional landforms are widespread in the Kanas River valley (Fig. 1).

3.1. Glacial depositional landforms

Glaciers have been retreating in the Kanas River valley since the Little Ice Age (LIA), and the imprints of recent glacier retreat (during the past three decades) are very clear along the margins of modern glaciers. This includes fresh moraines beyond the terminus of the Kanas glacier, extending from 2460 m asl to 2416 m asl and distributed along an 800 m length of the valley.

From the modern moraine complex of the Kanas glacier (2416 m asl) to the lower regions of the valley at1200 m asl, there are four sets of moraines in this drainage (Fig. 1). The first and innermost moraine complex occurs between 0.8 and 3 km from the terminus of the Kanas glacier and at an altitude of between 2416 m asl (1980 position) to 2250 m asl. The glaciation that produced this moraine complex has been named the Youyifeng glaciation by Liu and Wang (1983). The complex consists of several end moraines separated by areas several meters lower, and the moraines have incipient weathering but no soil development. Shrubs and some coniferous trees have colonized the outmost margin of the moraine complex, and the trees are mainly firs with trunk diameters less than 10 cm. The main lithology of the till clasts is granite.

The second set of moraines occurs at about 1800 m asl, consists of three end moraines, and is about 18 km down valley from the moraine complex of the Youyifeng glaciation. The height of the innermost end moraine is about 20–40 m, of the middle is about 100 m, and of the outermost is about 60 m (Cui et al., 1992). Clasts in the till are mainly granite and schist, and boulders on the moraine surface show signs of weathering. The moraines have a 20–30 cm-thick dark brown soil that supports coniferous forest.

The Kanas River is blocked by this moraine complex, and a moraine-dammed glacial lake of ~9 km^2 developed behind it (Fig. 2). The local people call this lake “Akekule Lake” and this glaciation has therefore been named the Akekule glaciation (Cui et al., 1992). Two lateral moraines are preserved between the Youyifeng and the Akekule moraine complexes, and they occur about 60–100 m and 150–200 m above the Kanas River. Field investigation and geomorphic relationships indicate that the lower lateral moraine was formed during the Akekule glaciation.

The third set of moraines in this valley is located at the outlet of Kanas Lake and extends about 3.5 km from north to south along the Kanas River. The glaciation producing this moraine complex has therefore been named the Kanas glaciation (Liu and Wang, 1983; Cui et al., 1992). This moraine complex is the largest of the succession and consists of more than ten end moraines that have well-developed gray-cinnamon soil and abundant vegetation cover. These moraines have crests about 20–40 m above the Kanas River and weathered granite boulders 1–2 m in diameter. The features of the glacial landforms have led to the subdivision of the moraines into three subsets (III_1, III_2 and III_3) (Fig. 3). The III_1 moraine complex is the largest and consists of 7–9 end moraines at an altitude between 1370 and 1400 m asl and the relative height between them is 5–10 m. The III_2 moraine complex is 2.5–3.0 km from the outlet of the Kanas Lake. It consists of 3 end moraines that have a gray-cinnamon soil with a depth of ~25 cm. The III_3 moraine complex is about 3.5 km from the outlet of the Kanas Lake, and consists of 3–4 end moraines with widths of about 400–500 m. They are overlain by ~50 cm of loess in which a 20 cm-thick gray-

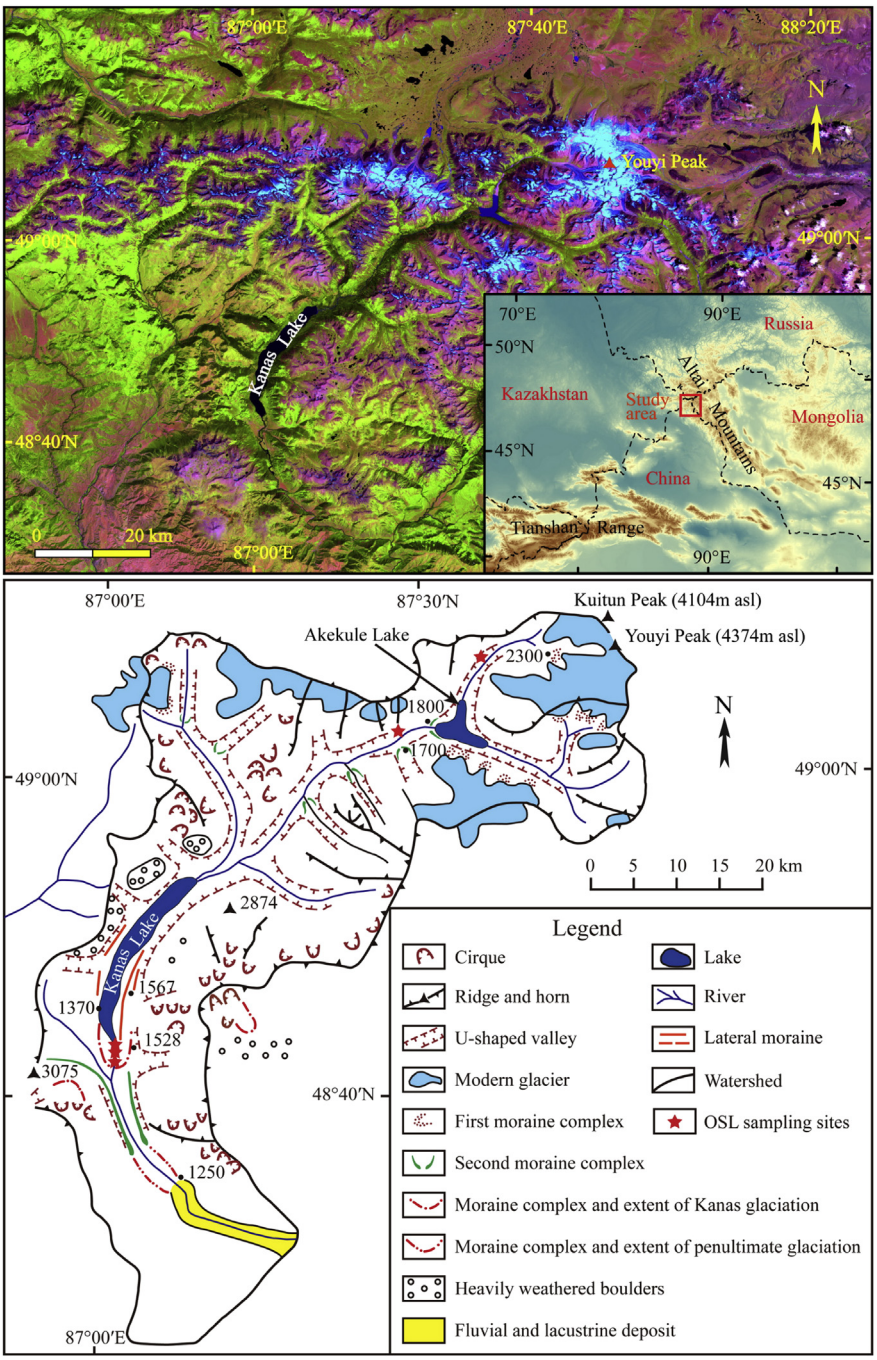

Fig. 1. Geomorphological map of the Kanas River valley (low one modified from Cui et al., 1992).

cinnamon soil has developed. An outwash with horizontal bedding corresponding to these moraines is preserved down valley. The lithologies of the till clasts are granite, schist, sandstone, shale and limestone. Geomorphic relationships indicate that lateral moraines that preserved discontinuously in the main glacial trough between Akekule Lake and the Kanas Lake were also formed during the Kanas glaciations, as was a higher lateral moraine between the first moraine complex and Akekule Lake.

The outermost moraine complex (the fourth moraine complex) is located at an altitude of between 1600 and 1200 m asl, about 18–20 km from the outlet of Kanas Lake. Glacial landforms here have undergone significant erosional modification since they were formed, the moraine complex is presented by benches of till about 200 m above the Kanas River that have deeply weathered granite and schist boulders on their surfaces. The degree of the weathering compared to that on the moraine complex of the Kanas glaciaiton indicates that this moraine complex represents an older glaciation. Along the road, till clasts in road cuts have lithologies similar to those in deposits of the Kanas glaciations, granite, schist, sandstone, shale and limestone. In addition, there are some highly weathered granite erratic boulders 1–2 m in diameter on ridges of pre-Cambrian phyllite bedrock at an altitude of between 1850 and 2150 m asl. Unfortunately, no original glacial landforms are preserved. Therefore, it is reasonable to conclude that the deeply weathered erratic boulders are relicts of a much older glaciation in this drainage.

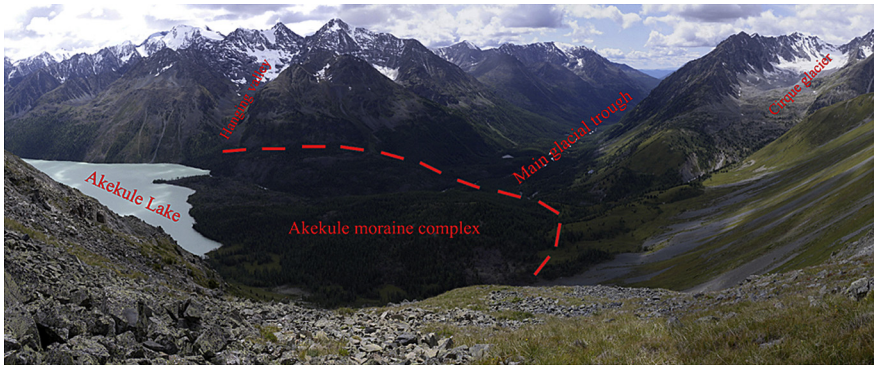

Fig. 2. Akekule moraine-dammed lake and Akekule moraine complex.

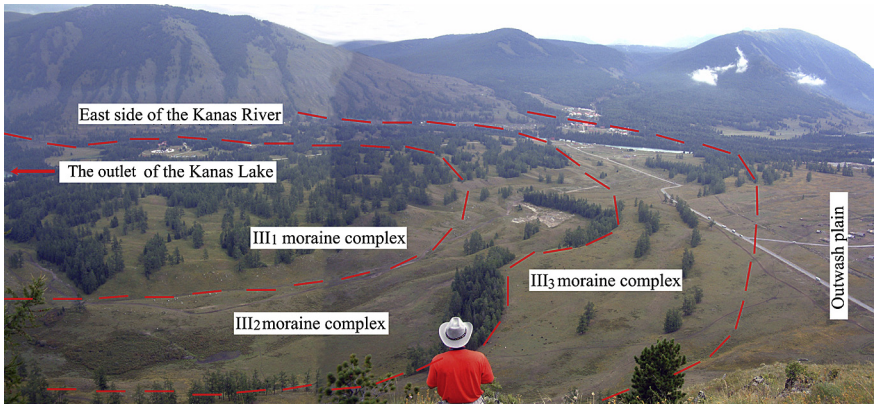

Fig. 3. Photo of the end moraines of the Kanas glaciation at the outlet of the Kanas Lake (provided by Dr. Xu Xiangke).

3.2. *Glacial erosional landforms*

Glacial troughs are the most outstanding glacial erosional landform in this drainage. The whole Kanas valley is a well-developed glacial trough, extending ~100 km from the terminus of the Kanas glacier at 2460 m asl to an altitude of about 1200 m asl. Hanging valleys, which are also well developed on both sides of the Kanas glacial trough, demonstrate that past glaciers in the Kanas valley included large compound valley glaciers. Cirques are another outstanding erosional landform in this valley (Fig. 4). Most of the cirques occur at an altitude of 2600–2700 m asl. Other erosional features, including horns, arêtes, roche moutonnées and polished bedrock are also well developed in this drainage.

4. Methods

To constrain the chronology of glaciation in the Kanas River valley, five samples for OSL dating were collected from natural or man-made sections. Two samples were collected from the lateral moraine in the headwaters (K-1 collected from the higher lateral

Fig. 4. Cirques located to the southwest outlet of the Kanas Lake (48°40′N, 86°55′E. ~2600 m asl).

moraine between the Youyifeng and the Akekule moraine complexes and K-2 collected from the lateral moraine, about 2 km downward to the Akekule lake) and the other three samples collected from the end moraines of the Kanas glaciation (Figs. 1 and 5). The samples were all taken from fluvioglacial deposits (sand lenses) that were sandwiched between till in the moraines. The samples were collected using metal tubes to ensure that they were not exposed to light.

The samples were analyzed in the OSL chronology laboratory at the Qinghai Institute of Salt Lakes, Chinese Academy of Sciences (CAS), Xining. The samples in the metal tubes were sub-sampled under safe red laboratory light. The outer 2–3 cm of each end of each sample was removed and the interior was chemically treated and then sieved to collect the 38–63 μm size fraction which was then treated following the procedures described by Ou et al. (2010), Zhang et al. (2012) and Zhao et al. (2012). The material in the 38–63 μm size fraction was etched with 35% hydrofluorosilicic acid (H_2SiF_6) for about 2 weeks to dissolve feldspars and then with 10% HCl to remove fluoride precipitates. The purity of treated quartz grains was checked by IR stimulation to ensure that feldspar contamination had been efficiently removed. Samples with obvious IRSL (infrared stimulated luminescence) signals were re-treated with H_2SiF_6 to avoid age underestimation (Lai and Brückner, 2008). Quartz grains were then mounted on stainless steel discs (10 mm in diameter) using silicone oil.

OSL measurements were performed on a Risø TL/OSL-DA-20 reader. To keep any residual IRSL signals from affecting the equivalent dose (D_e) estimation, a post-IR dating procedure was applied. The quartz discs were stimulated by infrared stimulation for 100 s at 0 °C before blue light stimulation using the double-SAR protocol (Banerjee et al., 2001). Based on previous studies (Ou et al., 2010; Zhang et al., 2012; Zhao et al., 2012), 260 °C (10 s) was selected as the preheat temperature for the blue light stimulation experiment. Stimulation with blue LEDs ($\lambda = 470 \pm 20$ nm) lasted for 40 s at 130 °C. The OSL signal was detected using a 9235QA photomultiplier tube with a 7.5 mm thick Hoya U-340 detection filter. Fig. 6 shows typical OSL decay curves for sample K-1 for natural dose (N), test dose (TD = 14.9 Gy), and regeneration doses of 209 Gy and 0 Gy. The curves show that the OSL signal decreases very quickly in the first second of stimulation, indicating that the signal is fast component dominant. For most aliquots, the recycling ratios were acceptable, implying that the test dose corrected for sensitivity changes appropriately.

D_es were determined using both the single-aliquot regenerative-dose (SAR) protocol (Murray and Wintle, 2000) and the standardized growth curve (SGC) methods (Roberts and Duller, 2004; Lai, 2006). For each sample, 6 aliquots were used for D_e determination using the SAR protocol (Fig. 7), and the SGCs were constructed using the SAR data. Then, 16–18 additional aliquots were prepared and measured for the natural (L_N) and test dose (T_N) under the same conditions as those for the SAR procedure. The test dose corrected natural OSL signal level (L_N/T_N) was then matched with the SGC to obtain a D_e value. The D_es determined by SGC and SAR protocols are in agreement. The final D_e is the mean of SAR D_es and SGC D_es.

The concentrations of U and Th and the K content were determined by neutron activation analysis (NAA) at the China Institute of Atomic Energy, Beijing. The annual dose rate (D) was estimated from these radioactive elements, the samples' water contents and cosmic ray contribution (Prescott and Hutton, 1994). Ages were calculated using the following equation:

$$T = \frac{D_e}{D}$$

where D_e is the equivalent dose and the D is the annual dose rate.

5. Results and discussion

For each sample, systematic and random errors in the De value were evaluated and uncertainties in cosmic ray contribution, secular water content, concentrations of U and Th and K content were considered. Take these uncertainties into account, the total uncertainty for each sample was estimated. The details of the sample sites, parameters used in the calculations are listed in Table 1. The OSL dating results in this study indicate an age order for the moraines that is consistent with the geomorphic and stratigraphic order of the features as well as with the weathering and soil development sequence of the moraines. However, because some concerns have been raised about using OSL in glacial sediments, we first discuss OSL setting in glacial environments and demonstrate that the samples used here were well bleached, before discussing the wider implications of the OSL ages.

Fig. 5. Well-exposed glacial sediment section and OSL ages.

Table 1
OSL dating results and parameters used in calculations

Lab No.	Samples' locations and description					U (10^{-6})	Th (10^{-6})	*K* (%)	Water (%)	Dose rate (Gy/ka)	TD (Gy)	Age (ka)
	Longitude/E	Latitude/N	Altitude/m asl	Depth/m	Sample's description							
K-1	87°36′57.52″	49°07′42.31″	2352	0.3	Sand lenses in the higher lateral moraine between the Youyifeng and the Akekule moraine complexes	2.44 ± 0.23	9.70 ± 0.25	2.15 ± 0.08	2.38	3.92 ± 0.07	106.57 ± 2.01	27.2 ± 2.0
K-2	87°29′36.19″	49°02′47.89″	1834	0.8	Sand lenses in the lateral moraine downward (~2 km) to the Akekule lake	3.54 ± 0.21	15.88 ± 0.37	2.36 ± 0.07	8.83	4.53 ± 0.28	72.94 ± 4.43	16.1 ± 1.5
K-3	87°01′12.85″	48°41′50.36″	1380	0.6	Sand lenses in the III_2 moraine complex of the Kanas glaciation	3.11 ± 0.21	15.09 ± 0.35	1.69 ± 0.07	2.81	3.45 ± 0.24	164.5 ± 24.1	43.6 ± 6.7
K-5	87°02′09.95″	48°42′09.39″	1399	0.3	Sand lenses in the III_2 moraine complex of the Kanas glaciation	2.35 ± 0.21	9.40 ± 0.24	1.81 ± 0.07	8.83	3.50 ± 0.16	182.5 ± 25.8	52.1 ± 7.8
K-4	87°00′55.49″	48°41′32.22″	1378	0.4	Sand lenses in the III_3 moraine complex of the Kanas glaciation	2.04 ± 0.17	10.05 ± 0.25	1.84 ± 0.07	2.37	3.47 ± 0.16	253.4 ± 19.7	73.1 ± 6.6

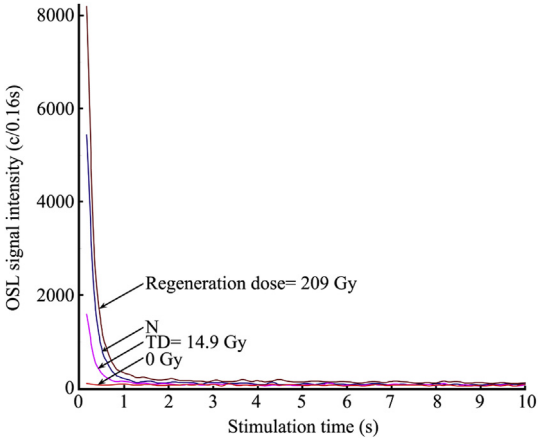

Fig. 6. OSL decay curves of natural dose (*N*), test dose (14.9 Gy), and regeneration doses of 209 Gy and 0 Gy for sample K-1.

5.1. Resetting OSL signals in glacial environments

An important assumption of the OSL dating technique is that the mineral grains were bleached before the sediments were deposited. After bleaching and deposition, luminescence signals are built up over time as a result of radiation emitted from natural radioactive elements and cosmic rays. Previous studies have shown that some glacigenic sediments are only partially bleached (Duller, 1994, 2006; Fuchs and Owen, 2008; Thrasher et al., 2009), and that the possibility of exposure and bleaching of the grains decreases in order from supraglacial debris, to englacial debris, to basal debris. This is consistent with the structure and movement of mountain glaciers (Shi et al., 1989) and formation models for lateral moraines (Small, 1983), which indicate that glacigenic sediments of alpine glaciers may have opportunities for exposure. However, fluvioglacial deposits should be better bleached than tills (Fuchs and Owen, 2008; Thrasher et al., 2009). Although some studies have indicated that the glacigenic sediments can potentially be bleached (Ou et al., 2010; Zhang et al., 2012). Zhao et al. (2012) working in the eastern segment of the Tianshan range has argued that fluvioglacial deposits (sand lenses) are much more suitable for dating than tills, if they are available.

D_e frequency histograms have been used to detect partially bleached sediments by some researchers (Murray et al., 1995; Olley et al., 1998, 1999; Bøe et al., 2007; Ou et al., 2010; Zhang et al., 2012; Zhao et al., 2012). For well-bleached sediments, the frequency histograms have a narrow and almost normal distribution, whereas, partially-bleached sediments have frequency histograms with a broad distribution and are skewed towards the larger D_e values

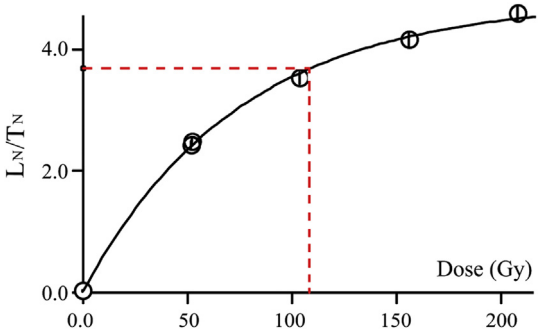

Fig. 7. Growth curve of single-aliquot regenerative-dose for sample K-1.

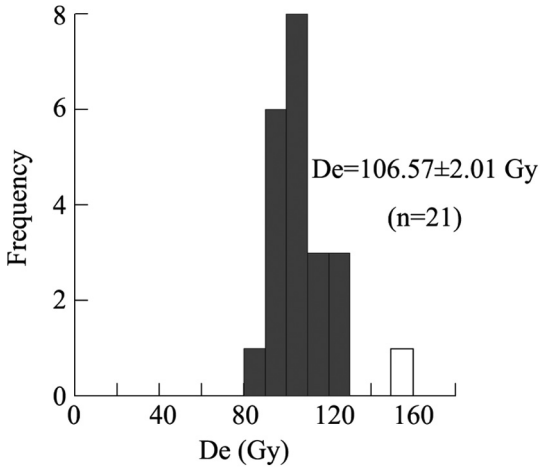

Fig. 8. D_es histogram of sample K-1. The empty column (aliquot with and abnormally high dose) is excluded when calculating the average D_e.

(Duller, 2004; Fuchs et al., 2007). The D_e frequency histograms obtained for our samples have a narrow and nearly symmetric shape (Fig. 8), indicating that sufficient bleaching of the quartz grains occurred in the fluvioglacial samples used in this study.

5.2. Quaternary glaciations and glacial landform evolution

Quaternary glacial successions in the Kanas River valley provide a promising opportunity for understanding palaeo-environmental variations in this segment of the Altai Mountains, and numerical ages provide a temporal framework for examining the glacial landform evolution. Ages determined previously using OSL, ^{14}C and ESR from deposits in this valley (Cui et al., 1992; Xu et al., 2009; Xu, 2010) allow for comparisons with our dating results from glaciofluvial deposits (Table 2). A comparison of the dates and other palaeoclimate records demonstrates that there has been a complex and long history of landform evolution in this drainage (Figs. 9 and 10).

region in the 13th–19th centuries (Agatova et al., 2012). In addition, lichenometric results for three end moraines close to modern glaciers in the headwaters of the Urumqi River in the Tianshan range, which is also under the influence of the mid-latitude westerly circulation, are 1538 ± 20 a AD, 1770 ± 20 a AD and 1871 ± 20 a AD (Chen, 1989). Although we have no absolute dates on the first moraine complex in the Kanas Valley, from its position and from the regional chronology we hypothesize that this first moraine complex was deposited during the LIA. Based on the pattern of glacial landforms, the Kanas glacier was about 13.8 km long at its maximum extent during this time.

Previous works showed that the special inorganic deposit, such as carbonate coating on glacial deposits (e.g. boulders) could be used to define the timing of glaciations (Cui et al., 1992; Yi et al., 1998, 2004). Cui et al. (1992) dated a carbonate coating that collected from boulder by ^{14}C to 4040 ± 80 a BP. This is consistent with ^{14}C ages for the Akkem stage (from 4900 to 4200 cal years BP) in the North Chuya range (Agatova et al., 2012). Based on this previous work and the consistency with the chronology in the adjacent area of the Russian Altai, we conclude that the Akekule glaciation is Neoglacial in age, and at this time, the Kanas glacier was up to 32 km long.

Previous work on the Kanas glaciation is controversial because of a potential lack of synchronicity with global records. Although it has often been assumed that mountain glaciations were occurring global synchronously (Broecker and Denton, 1990), there is increasing evidence that glacial advances varied regionally during the last glacial cycle, and that the local last glacial maximum (LGM_L) did not everywhere coincide with the temperature minimum during the global Last Glacial Maximum (LGM_G) (Mix et al., 2001; Clark et al., 2009), as first described by Gillespie and Molnar (1995). Since then, many studies in High Asia have tested and partially confirmed this view (Owen et al., 2002a, 2003; Zech et al., 2003; Finkel et al., 2003; Kamp Jr. et al., 2004; Zech et al., 2005; Abramowski et al., 2006; Zhao et al., 2007, 2009, 2010; Koppes et al., 2008; Gillespie et al., 2008; Shi et al., 2011; Heyman et al., 2011; Fu et al., 2013; Wang et al., 2013). Therefore, glaciations and landform evolution

Table 2
Dates of glacial sediments inferred from this study and previous works

Sampling sites	Dating techniques	Results and sources	Glaciations or MIS
The Akekule moraine complex	^{14}C	4040 ± 80 a BP Cui et al. (1992)	Neoglaciation
Higher lateral moraine between the Youyifeng and the Akekule moraine complexes; lateral moraine downward (~2 km) to the Akekule lake	OSL	27.2 ± 2.0 ka (K-1), 16.1 ± 1.5 ka (K-2) this study	MIS 2
III_1 moraine complex of the Kanas glaciation	OSL	28.2 ± 3.3 ka (KNS07-50) Xu et al. (2009)	MIS 2
III_2 moraine complex of the Kanas glaciation	OSL	34.4 ± 4.2 ka (KNS07-67); 38.1 ± 4.5 ka (KNS07-68) Xu et al. (2009)	MIS 3a
		43.6 ± 6.7 ka, 52.1 ± 7.8 ka this study	mid-MIS 3
III_3 moraine complex of the Kanas glaciation	OSL	49.9 ± 5.4 ka (KNS07-57) Xu et al. (2009)	MIS 3b
		73.1 ± 6.6 ka this study	MIS 4
The fourth set of moraine complex	ESR	125 ± 12 ka (KNS08-33), 156 ± 15 ka (KNS08-34), 167 ± 16 ka (KNS08-35), 123 ± 18 ka (KNS08-41), 137 ± 14 ka (KNS08-42) Xu (2010)	MIS 6

The pattern of moraines most commonly found in Western China, has a first set of the moraines close to but beyond the modern glacier that were deposited during the LIA (Shi et al., 2006, 2011). The ^{14}C chronology of glacial sequences in the North Chuya range, northeast of the Youyi Peak area in Russia provides a good reference for discussing the timing of the first moraine complex in this drainage. The ^{14}C chronology of the Aktru glacial stage in the North Chuya range shows that LIA glacial advances occurred in this related to the Kanas glaciation must be discussed in detail before drawing any paleoclimatic conclusions.

Based on available OSL ages (Xu et al., 2009; Xu, 2010 and this study), the multiple end moraines of the Kanas glaciation were deposited during the last glaciation. According to the features of Kanas moraine complex, the dates could be divided into three clusters. They are 16.1–28.2 ka, 38.1–52.1 ka and 73.1 ± 6.6 ka. This is similar to the glacier development pattern reported for the Tumur

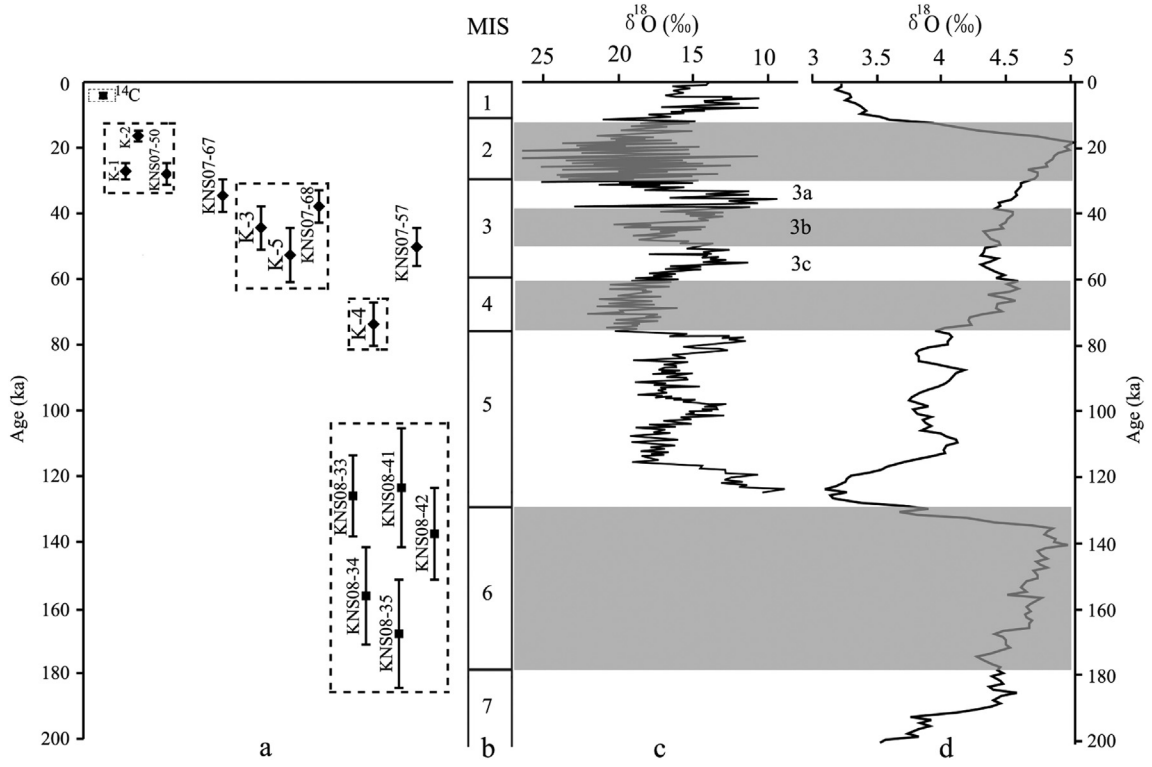

Fig. 9. A comparison of Quaternary glacial chronology in the Kanas River valley with different records. (a) dating results and their errors; (b) Marine oxygen isotope stage (MIS); (c) the $\delta^{18}O$ record of the Guliya ice core (modified after Yao et al., 1997); (d) the $\delta^{18}O$ record of the 57 globally distributed benthic sediments (modified after Lisiecki and Raymo, 2005).

Peak area of the Tianshan range by Zhao et al. (2010). The first cluster of ages (16.1–28.2 ka) indicate that the III_1 moraine complex was deposited during the late period of the last glaciation, corresponding to MIS 2. The III_2 moraine complex ages (38.1–52.1 ka) indicate that it was deposited during the last interstadial, corresponding to mid-MIS 3, and the glacier during this period was slightly larger than that during MIS 2. The age of the III_3 moraine complex (73.1 ± 6.6 ka; MIS 4) demonstrates that the LGM_L occurred in the early period of the last glaciation rather than during the LGM_G during MIS 2. The glacial landforms show that the Kanas glacier was ~100 km long at its maximum extent during the last glaciation.

Climatic conditions during the last glaciation have been reconstructed in several ways. Based on geomorphology, previous studies (Liu and Wang, 1983; Cui et al., 1992) have suggested that the cirques, whose floors are located at an altitude between 2600 and 2700 m asl were formed during the last glaciation. This leads them to conclude that the ELA was lowered about 600–700 m during last glaciation. Shi et al. (2000, 2006) proposed that the climate was cold and dry during the last glacial cycle and Shi et al. (2000) inferred that the humidity during MIS 4 was higher than that during MIS 2 in western China, especially in westerly circulation areas. This may provide an explanation for the LGM_L occurring during MIS 4 rather than MIS 2 in this region. The existence of a glacial expansion during MIS 3 is counter to the general global record, however, the Guliya ice core record for MIS 3 (58–32 ka) (Yao et al., 1997) includes a marked cold period during mid-MIS 3 (Fig. 9c). In addition, geomorphology and sedimentology research has shown that high lake levels and large fresh-water lakes have been present in the northwestern part of the Qinghai-Xizang Plateau and in the arid areas of Central Asia since mid-MIS 3 (Li et al., 1998, 2008; Zhang et al., 2002, 2004; Herzschuh, 2006). Together, these proxies suggest that a cold and humid climate prevailed in areas influenced by the westerly circulation during mid-MIS 3, which is consistent with a glacial advance in the Kanas River valley at that time. In addition, recent geomorphological and chronological evidence shows that glacial advances also occurred during MIS 3 in other mountainous areas in Central Asia (Zech et al., 2005; Abramowski et al., 2006; Gillespie et al., 2008; Koppes et al., 2008; Zhao et al., 2009, 2010; Zech, 2012). Therefore, it is reasonable to conclude that a cold-humid climate during mid-MIS 3

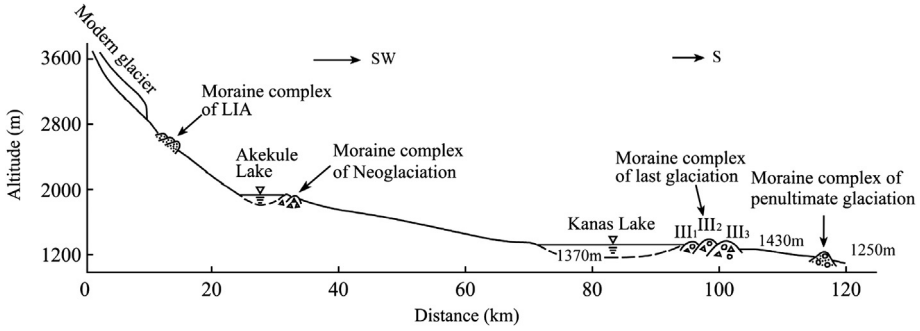

Fig. 10. Longitudinal profile of the Kanas River valley showing the moraine complexes of the different glaciations (modified after Cui et al., 1992).

caused a glacial advance in the Kanas River valley that was slightly larger than the advance during MIS 2 in this drainage.

The fourth moraine complex in the Kanas River valley has previously been dated with ESR techniques using germanium (Ge) centers in glacial quartz grains by Xu (2010). Previous studies indicate that Ge centers are sensitive to ultraviolet light, sunlight and grinding (Tanaka et al., 1985; Buhay et al., 1988; Jin et al., 1991; Ye et al., 1993, 1998; Walther and Zilles, 1994; Rink, 1997). ESR dating techniques have been successful in determining the ages of some glacial deposits and important results have been obtained (Yi et al., 2002; Zhou et al., 2002a, b; Zhao et al., 2006, 2009, 2010; Xu and Zhou, 2009; Wang et al., 2011). Five ESR dates were obtained by Xu (2010) from the fourth moraine complex (Figs. 9 and 10), with ages of 125 ± 12 ka (KNS08-33), 156 ± 15 ka (KNS08-34), 167 ± 16 ka (KNS08-35), 123 ± 18 ka (KNS08-41), and 137 ± 14 ka (KNS08-42), which are equivalent to MIS 6. These dates indicate that the fourth moraine complex was deposited during the penultimate glaciation. After this glaciation, the glacial landforms have been undergone a long period of erosion, and so the present landscape is not a good indicator of the landscape directly after glaciation. Based on the location of the fourth moraine complex, the Kanas glacier was at least ~120 km long during the MIS glaciation.

In addition to the fourth moraine complex, erratic granite boulders found at an altitude of between 1850 and 2150 m asl on both sides of the Kanas River with an even greater degree of weathering than those on the fourth moraine complex may represent and even older glaciation in this drainage. Studies of the oldest glaciations in the Qinghai-Xizang Plateau and its bordering areas, and as well as in the Tianshan range (Zhou et al., 2002a, 2006; Owen et al., 2006; Wang et al., 2006; Zhao et al., 2006, 2009), lead us to suggest the possibility that these weathered erratic may record glaciations in this drainage during MIS 12, however, additional research is needed to test this hypothesis.

6. Conclusion

Four sets of moraines occur in the Kanas River valley, Altai Mountains. Based on available dating results (^{14}C, OSL and ESR) and geomorphic relationships, the moraines close but beyond the modern glacial landforms were deposited during the LIA, the Akekule moraine complex was formed during the Neoglacial, the multiple end moraines of the Kanas glaciation were deposited in the last glacial cycle during MIS 2–4, and the outermost moraine complex was deposited during the penultimate glaciation, corresponding to MIS 6.

The glacial landforms indicate that the ancient Kanas glaciers at their maximum extensions during the LIA, Neoglacial, last glaciations and penultimate glaciations were 13.8 km, 32 km, ~100 km, and ~120 km long respectively. The landforms of the Kanas glaciation show that three large glacial advances occurred during the last glaciation, with ages equivalent to MIS 2, mid-MIS 3 and MIS 4. Thus in the Kanas River valley, a glacier which was slightly larger than that during the LGM_G (MIS 2) occurred in mid-MIS 3. The LGM_L occurred during the early period of the last glaciation (MIS 4) rather than LGM_G (MIS 2). Evidence for an even more extensive and earlier glaciation requires further research to establish the timing of this event.

Acknowledgements

We thank Wang Feiteng, Li Huilin, Kang Jian and Sun Jizhou for their fieldwork assistance. Zhang Jingran and Zhang Biao helped date and analyze the samples in the OSL chronology laboratory, Qinghai Institute of Salt Lakes, CAS, Xining. Xu Xiangke offered the fieldwork photos and some useful comments and suggestions. This work was supported by National Natural Science Foundation of China (Nos. 41071010, 41230743, 41271093), the Knowledge Innovation Project of the CAS (Nos. KZCX2-EW-QN304 and KZCX2-YW-GJ04) and the Program of State Key Laboratory of Cryospheric Sciences (No. SKLCS-ZZ-20120003). Harbor's work on this project was supported by Purdue University.

References

Abramowski, U., Bergau, A., Seebach, D., Zech, R., Glaser, B., Sosin, P., Kubik, P.W., Zech, W., 2006. Pleistocene glaciations of Central Asia: results from ^{10}Be surface exposure ages of erratic boulders from the Pamir (Tajikistan), and the Alay–Turkestan range (Kyrgyzstan). Quaternary Science Reviews 25, 1080–1096.

Agatova, A.R., Nazarov, A.N., Nepop, R.K., Rodnight, H., 2012. Holocene glacier fluctuations and climate changes in the southeastern part of the Russian Altai (South Siberia) based on a radiocarbon chronology. Quaternary Science Reviews 43, 74–93.

Banerjee, D., Murray, A.S., Bøtter-Jensen, L., Lang, A., 2001. Equivalent dose estimation using a single aliquot of polymineral fine grains. Radiation Measurements 33, 73–94.

Benn, D.I., Evans, D.J.A., 2010. Glacier and Glaciation, second ed. Hodder Education, London, pp. 1–802.

Bøe, A.G., Murray, A., Dahl, S.O., 2007. Resetting of sediments mobilised by the LGM ice-sheet in southern Norway. Quaternary Geochronology 2, 222–228.

Broecker, W.S., Denton, G.H., 1990. The role of ocean-atmosphere reorganizations in glacial cycles. Quaternary Science Reviews 9, 305–341.

Buhay, W.M., Schwarcz, H.P., Grün, R., 1988. ESR dating of fault gouge: the effect of grain size. Quaternary Science Reviews 7, 515–522.

Chen, J.Y., 1989. Preliminary researches on lichenometric chronology of Holocene glacial fluctuations and on other topics in the headwater of Urumqi River, Tianshan Mountains. Science in China (Series B) 32, 1487–1500.

Clark, P.U., Dyke, A.S., Shakun, J.D., Carlson, A.E., Clark, J., Wohlfarth, B., Mitrovica, J.X., Hostetler, S.W., McCabe, A.M., 2009. The last glacial maximum. Science 325, 710–714.

Cui, Z.J., Yi, C.L., Yan, J.F., 1992. Quaternary glaciations in the Halasi River catchment and its surroundings in the Altai Mountains in Xingjiang, China (in Chinese with English abstract). Journal of Glaciology and Geocryology 14, 342–351.

Duller, G.A.T., 2004. Luminescence dating of quaternary sediments: recent developments. Journal of Quaternary Science 19, 183–192.

Duller, G.A.T., 1994. Luminescence dating of poorly bleached sediments from Scotland. Quaternary Science Reviews 13, 521–524.

Duller, G.A.T., 2006. Single grain optical dating of glacigenic deposits. Quaternary Geochronology 1, 296–304.

Ehlers, J., Gibbard, P.L., Hughes, P.D., 2011. Quaternary Glaciations – Extent and Chronology. In: A Closer Look, vol. 15. Elsevier, Amsterdam, pp. 1–1108.

Embleton, C., King, C.A.M., 1975. Glacial Geomorphology. Edward Arnold, London, pp. 1–573.

Finkel, R.C., Owen, L.A., Barnard, P.L., Caffee, M.W., 2003. Beryllium-10 dating of Mount Everest moraines indicates a strong monsoonal influence and glacial synchroneity throughout the Himalaya. Geology 31, 561–564.

Fu, P., Stroeven, A.P., Harbor, J.M., Hättestrand, C., Heyman, J., Caffee, M.W., Zhou, L.P., 2013. Paleoglaciation of Shaluli Shan, southeastern Tibetan Plateau. Quaternary Science Reviews 64, 121–135.

Fuchs, M., Owen, L.A., 2008. Luminescence dating of glacial and associated sediments: review, recommendations and future directions. Boreas 37, 636–659.

Fuchs, M., Woda, C., Bürkert, A., 2007. Chronostratigraphy of a sedimentary record from the Hajar mountain range in north Oman: implications for optical dating of insufficiently bleached sediments. Quaternary Geochronology 2, 202–207.

Gillespie, A.R., Burke, R.M., Komatsu, G., Bayasgalan, A., 2008. Chronology of late Pleistocene glaciers in Darhad Basin, northern Mongolia. Quaternary Research 69, 169–187.

Gillespie, A.R., Molnar, P., 1995. Asynchronism of maximum advances of mountain and continental glaciations. Reviews of Geophysics 33, 311–364.

Herzschuh, U., 2006. Palaeo-moisture evolution in monsoonal Central Asia during the last 50000 years. Quaternary Science Reviews 25, 163–178.

Heyman, J., Stroeven, A.P., Caffee, M.W., Hättestrand, C., Harbor, J.M., Li, Y.K., Alexanderson, H., Zhou, L.P., Hubbard, A., 2011. Palaeoglaciology of Bayan Har Shan, NE Tibetan Plateau: exposure ages reveal a missing LGM expansion. Quaternary Science Reviews 30 (15–16), 1988–2001.

Jin, S.Z., Deng, Z., Huang, P.H., 1991. Study on optical effects of quartz E' center in loess. Chinese Science Bulletin 36, 1865–1870.

Kamp Jr., U., Haserodt, K., Shroder Jr., J.F., 2004. Quaternary landscape evolution in the eastern Hindu Kush, Pakistan. Geomorphology 57, 1–27.

Koppes, M., Gillespie, A.R., Burke, R.M., Thompson, S., Stone, J., 2008. Late Quaternary glaciation in the Kyrgyz Tien Shan. Quaternary Science Reviews 27, 846–866.

Lai, Z.P., 2006. Testing the use of an OSL standardised growth curve (SGC) for D_e determination on quartz from the Chinese loess Plateau. Radiation Measurements 41, 9–16.

Lai, Z.P., Brückner, H., 2008. Effects of feldspar contamination on equivalent dose and the shape of growth curve for OSL of silt-sized quartz extracted from Chinese loess. Geochronometria 30, 49–53.

Li, S.J., Qu, R.K., Zhu, Z.Y., Li, B.Y., 1998. A carbonate content record of late Quaternary climate and environment changes from lacustrine core TS95 in Tianshuihai lake basin, northwestern Qinghai–Xizang (Tibet) Plateau (in Chinese with English abstract). Journal of Lake Sciences 10, 58–65.
Li, S.J., Zhang, H.L., Shi, Y.F., Zhu, Z.Y., 2008. A high resolution MIS 3 environmental change record derived from lacustrine deposit of Tianshuihai lake, Qinghai – Tibet Plateau (in Chinese with English abstract). Quaternary Sciences 28, 122–131.
Lisiecki, L.E., Raymo, M.E., 2005. A Pliocene-Pleistocene stack of 57 globally distributed benthic $\delta^{18}O$ records. Paleoceanography 20, PA1003. http://dx.doi.org/10.1029/2004PA001071.
Liu, C.H., Wang, L.L., 1983. Traces of ancient glaciations and their division in the Quaternary at the drainage basin of Halasi River in the Altay Shan of China (in Chinese with English abstract). Journal of Glaciology and Cryopedology 5, 39–47.
Liu, C.H., You, G.X., Pu, J.C., 1982. Glacier Inventory of China II: Altay Mountains (in Chinese). Lanzhou Institute of Glaciology and Cryopedology, Academia Sinica, Lanzhou, pp. 1–87.
Mix, A.C., Bard, E., Schneider, R., 2001. Environmental processes of the ice age: land, oceans, glaciers (EPILOG). Quaternary Science Reviews 20, 627–657.
Murray, A.S., Olley, J.M., Caitcheon, G.G., 1995. Measurement of equivalent doses in quartz from contemporary water-lain sediments using optically stimulated luminescence. Quaternary Science Reviews 14, 365–371.
Murray, A.S., Wintle, A.G., 2000. Luminescence dating of quartz using an improved single-aliquot regenerative-dose protocol. Radiation Measurements 32, 57–73.
Olley, J.M., Caitcheon, G.G., Murray, A.S., 1998. The distribution of apparent dose as determined by optically stimulated luminescence in small aliquots of fluvial quartz: implications for dating young sediments. Quaternary Science Reviews 17, 1033–1040.
Olley, J.M., Caitcheon, G.G., Roberts, R.G., 1999. The origin of dose distributions in fluvial sediments, and the prospect of dating single grains from fluvial deposits using optically stimulated luminescence. Radiation Measurements 30, 207–217.
Ou, X.J., Xu, L.B., Lai, Z.P., Long, H., He, Z., Fan, Q.S., Zhou, S.Z., 2010. Potential of quartz OSL dating on moraine deposits from eastern Tibetan Plateau using SAR protocol. Quaternary Geochronology 5, 257–262.
Owen, L.A., Caffee, M.W., Bovard, K.R., Finkel, R.C., Sharma, M.C., 2006. Terrestrial cosmogenic nuclide surface exposure dating of the oldest glacial successions in the Himalayan orogen: Ladakh range, northern India. Geological Society of America Bulletin 118, 383–392.
Owen, L.A., Finkel, R.C., Caffee, M.W., 2002a. A note on the extent of glaciation throughout the Himalaya during the global Last Glacial Maximum. Quaternary Science Reviews 21, 147–157.
Owen, L.A., Finkel, R.C., Ma, H.Z., Spencer, J.Q., Derbyshire, E., Barnard, P.L., Caffee, M.W., 2003. Timing and style of late Quaternary glaciation in northeastern Tibet. Geological Society of America Bulletin 115, 1356–1364.
Owen, L.A., Kamp, U., Spencer, J.Q., Haserodt, K., 2002b. Timing and style of Late Quaternary glaciation in the eastern Hindu Kush, Chitral, northern Pakistan: a review and revision of the glacial chronology based on new optically stimulated luminescence dating. Quaternary International 97/98, 41–55.
Prescott, J.R., Hutton, J.T., 1994. Cosmic ray contributions to dose rates for luminescence and ESR dating: large depths and long-term time variations. Radiation Measurements 23, 497–500.
Rink, W.J., 1997. Electron spin resonance (ESR) dating and ESR applications in Quaternary science and archaeometry. Radiation Measurements 27, 975–1025.
Roberts, H.M., Duller, G.A.T., 2004. Standardised growth curves for optical dating of sediment using multiple-grain aliquots. Radiation Measurements 38, 241–252.
Shi, Y.F., Huang, M.H., Yao, T.D., Deng, Y.X. (Eds.), 2000. Glaciers and their Environments in China – The Present, Past and Future. Science Press, Beijing, pp. 1–410 (in Chinese).
Shi, Y.F., Cui, Z.J., Li, J.J. (Eds.), 1989. Problems on Quaternary Glaciation and Environments in Eastern China. Science Press, Beijing, pp. 11–31 (in Chinese).
Shi, Y.F., Cui, Z.J., Su, Z., 2006. The Quaternary Glaciations and Environmental Variations in China (in Chinese with English summary). Hebei Science and Technology Publishing House, Shijiazhuang, pp. 1–618.
Shi, Y.F., Zhao, J.D., Wang, J., 2011. New Understanding of Quaternary Glaciations in China (in Chinese). Shanghai Popular Science Press, Shanghai, pp. 1–213.
Small, R.J., 1983. Lateral moraines of glacier De Tsidjiore Nouve: form, development and implications. Journal of Glaciology 29, 250–259.
Tanaka, T., Sawada, S., Ito, T., 1985. ESR dating of late Pleistocene near-shore and terrace sands in southern Kanto, Japan. In: Ikeya, M., Miki, T. (Eds.), ESR Dating and Dosimetry. Ionics, Tokyo, pp. 275–280.
Thrasher, I.M., Mauz, B., Chiverrell, R.C., Lang, A., 2009. Luminescence dating of glaciofluvial deposits: a review. Earth-Science Reviews 97, 133–146.
Thompson, L.G., Yao, T., Davis, M.E., Henderson, K.A., Thompson, E.M., Lin, P.N., Beer, J., Synal, H.A., Cole-Dai, J., Bolzan, J.F., 1997. Tropical climate instability: the last glacial cycle from a Qinghai–Tibetan ice core. Science 276, 1821–1825.
Walther, R., Zilles, D., 1994. ESR studies on bleached sedimentary quartz. Quaternary Science Reviews 13, 611–614.
Wang, J., Raisbeck, G., Xu, X.B., Yiou, F., Bai, S.B., 2006. In situ cosmogenic ^{10}Be dating of the Quaternary glaciations in the southern Shaluli mountain on the Southeastern Tibetan Plateau. Science in China (Series D) 49, 1291–1298.
Wang, J., Zhou, S.Z., Zhao, J.D., Zheng, J.X., Guo, X.Z., 2011. Quaternary glacial geomorphology and glaciations of Kongur Mountain, eastern Pamir, China. Science China Earth Sciences 54, 591–602.
Wang, J., Kassab, C., Harbor, J.M., Caffee, M.W., Cui, H., Zhang, G.L., 2013. Cosmogenic nuclide constraints on late Quaternary glacial chronology on the Dalijia Shan, northeastern Tibetan Plateau. Quaternary Research 79, 439–451.
Wang, L.L., Liu, C.H., Kang, X.C., You, G.X., 1983. Fundamental features of modern glaciers in the Altay Shan of China (in Chinese with English abstract). Journal of Glaciology and Cryopedology 5, 27–38.
Wu, J.L., Wang, S.M., Shi, Y.F., Lei, J., 2000. Temperature estimation by oxygen-stable record over the past 200 ka in Zoige Basin. Science in China (Series D) 43, 577–586.
Xu, L.B., Ou, X.J., Lai, Z.P., Zhou, S.Z., Wang, J., Fu, Y.C., 2010. Timing and style of Late Pleistocene glaciation in the Queer Shan, northern Hengduan Mountains in the eastern Tibetan Plateau. Journal of Quaternary Science 25, 957–966.
Xu, L.B., Zhou, S.Z., 2009. Quaternary glaciations recorded by glacial and fluvial landforms in the Shaluli Mountains, southeastern Tibetan Plateau. Geomorphology 103, 268–275.
Xu, X.,K., Yang, J.,Q., Dong, G.,C., Wang, L.Q., Miller, L., 2009. OSL dating of glacier extent during the Last Glacial and the Kanas Lake basin formation in Kanas River valley, Altai Mountains, China. Geomorphology 112, 306–317.
Xu, X.K., 2010. Late Pleistocene Glacial Geomorphology and Dating in K'anas River Valley, Altai Mountains. Graduate University of Chinese Academy of Sciences, Beijing (in Chinese with English abstract). Unpublished Ph. D. thesis.
Yao, T.D., Thompson, L.G., Shi, Y.F., Qin, D.H., Jiao, K.Q., Yang, Z.H., Tian, L.D., Thompson, E.M., 1997. Climate variation since the last interglaciation recorded in the Guliya ice core. Science in China (Series D) 40, 662–668.
Ye, Y.G., Diao, S.B., He, J., Gao, J.C., Lei, X.Y., 1998. ESR dating studies of paleo-debris-flows deposition Dongchuan, Yunnan province, China. Quaternary Geochronology (Quaternary Science Reviews) 17, 1073–1076.
Ye, Y.G., He, J., Diao, S.B., Gao, J.C., 1993. Study on ESR ages of late Pleistocene coastal aeolian sands (in Chinese with English abstract). Marine Geology & Quaternary Geology 13 (3), 85–90.
Yi, C.L., Li, X.Z., Qu, J.J., 2002. Quaternary glaciation of Puruogangri – the largest modern ice field in Tibet. Quaternary International 97/98, 111–121.
Yi, C.L., Liu, K.X., Cui, Z.J., 1998. AMS dating on glacial tills at the source area of the Urumqi River in the Tianshan Mountains and its implications. Chinese Science Bulletin 43, 1749–1751.
Yi, C.L., Liu, K.X., Cui, Z.J., Jiao, K.Q., Yao, T.D., He, Y.Q., 2004. AMS radiocarbon dating of late Quaternary glacial landforms, source of the Urumqi River, Tien Shan – a pilot study of ^{14}C dating on inorganic carbon. Quaternary International 121, 99–107.
Zech, R., 2012. A late Pleistocene glacial chronology from the Kitschi-Kurumdu Valley, Tien Shan (Kyrgyzstan), based on ^{10}Be surface exposure dating. Quaternary Research 77, 281–288.
Zech, R., Abramowski, U., Glaser, B., Sosin, P., Kubik, P.W., Zech, W., 2005. Late Quaternary glacial and climate history of the Pamir Mountains derived from cosmogenic ^{10}Be exposure ages. Quaternary Research 64, 212–220.
Zech, W., Glaser, B., Abramowski, U., Dittmar, C., Kubik, P.W., 2003. Reconstruction of the Late Quaternary Glaciation of the Macha Khola valley (Gorkha Himal, Nepal) using relative and absolute (^{14}C, ^{10}Be, dendrochronology) dating techniques. Quaternary Science Reviews 22, 2253–2265.
Zhang, B., Ou, X.J., Lai, Z.P., 2012. OSL ages revealing the glacier retreat in the Dangzi valley in the eastern Tibetan Plateau during the Last Glacial Maximum. Quaternary Geochronology 10, 244–249.
Zhang, H.C., Peng, J.L., Ma, Y.Z., Chen, G.J., Feng, Z.D., Li, B., Fan, H.F., Chang, F.Q., Lei, G.L., Wünnemann, B., 2004. Late Quaternary palaeolake levels in Tengger Desert, NW China. Palaeogeography, Palaeoclimatology, Palaeoecology 211, 45–58.
Zhang, H.C., Wünnemann, B., Ma, Y.Z., Peng, J.L., Pachur, Hans-J., Li, J.J., Qi, Y., Chen, G.J., Fang, H.B., Feng, Z.D., 2002. Lake level and climate changes between 42000 and 18000 ^{14}C yr BP in the Tengger Desert, northwestern China. Quaternary Research 58, 62–72.
Zhao, J.D., Lai, Z.P., Liu, S.Y., Song, Y.G., Li, Z.Q., Yin, X.F., 2012. OSL and ESR dating of glacial deposits and its implications for glacial landform evolution in the Bogeda Peak area, Tianshan range, China. Quaternary Geochronology 10, 237–243.
Zhao, J.D., Liu, S.Y., He, Y.Q., Song, Y.G., 2009. Quaternary glacial chronology of the Ateaoyinake River Valley, Tianshan Mountains, China. Geomorphology 103, 276–284.
Zhao, J.D., Song, Y.G., King, J.W., Liu, S.Y., Wang, J., Wu, M., 2010. Glacial geomorphology and glacial history of the Muzart River valley, Tianshan range, China. Quaternary Science Reviews 29, 1453–1463.
Zhao, J.D., Zhou, S.Z., Liu, S.Y., He, Y.Q., Xu, L.B., Wang, J., 2007. A preliminary study of the glacier advance in MIS 3b in the western regions of China (in Chinese with English abstract). Journal of Glaciology and Geocryology 29, 233–241.
Zhao, J.D., Zhou, S.Z., He, Y.Q., Ye, Y.G., Liu, S.Y., 2006. ESR dating of glacial tills and glaciations in the Urumqi River headwaters, Tianshan Mountains, China. Quaternary International 144, 61–67.
Zhao, J.D., Shi, Y.F., Wang, J., 2011. Comparison between Quaternary glaciations in China and the marine oxygen isotope stage (MIS): an improved schema (in Chinese with English abstract). Acta Geographica Sinica 66 (7), 867–884.
Zhou, S.Z., Jiao, K.Q., Zhao, J.D., Zhang, S.Q., Cui, J.X., Xu, L.B., 2002a. Geomorphology of the Urumqi River Valley and the uplift of the Tianshan Mountains in Quaternary. Science in China (Series D) 45, 961–968.
Zhou, S.Z., Li, J.J., Zhang, S.Q., 2002b. Quaternary glaciation of the Bailang River Valley, Qilian Shan. Quaternary International 97/98, 103–110.
Zhou, S.Z., Wang, X.L., Wang, J., Xu, L.B., 2006. A preliminary study on timing of the oldest Pleistocene glaciation in Qinghai–Tibetan Plateau. Quaternary International 154/155, 44–51.
Zhou, S.Z., Xu, L.B., Colgan, P.M., Mickelson, D.M., Wang, X.L., Wang, J., Zhong, W., 2007. Cosmogenic ^{10}Be dating of Guxiang and Baiyu glaciations. Chinese Science Bulletin 52, 1387–1393.